The Investigation of Parachute Suspension Line Fluid-Structure Interactions using LS-DYNA® ICFD

Catherine P. Barry[1], Bradford G. Olson[1], Keith Bergeron[2],
David J. Willis[1], James A. Sherwood[1]
[1]*University of Massachusetts Lowell*
[2]*U.S. Army Natick Soldier Research, Development & Engineering Center*

Abstract

The U.S. Army uses autonomously guided parachute systems to deliver supplies to troops in the field. Each system consists, primarily, of a lightweight canopy, braided polyester suspension lines, and payload. As a system descends, the suspension lines generate and shed vortices as a result of the cross-flow of air, and these vortices induce fluctuating drag and lift forces. These fluctuating forces introduce system performance degradations, and the excited vibrations can often be heard for several kilometers. One method to assist in developing a fundamental understanding of the relationship between the suspension-line architecture, e.g. surface geometry and tensile and torsional stiffnesses, and the associated vortex-induced vibrations is the running of cyber-physical fluid dynamics (CPFD) experiments. The CPFD system consists of a rigid scale model of a section of the suspension line mounted on a servomotor within a wind tunnel. The servomotor accounts for the evolution in the torsional stiffnesses of the suspension line as a function of the degree of tensile force. The combination of the angle of attack, surface geometry, and axial tension determine the resulting vibration of the line. In the current research, the CPFD system is modeled using the LS-DYNA incompressible fluid dynamics (ICFD) solver, and is analyzed as a two-way FSI problem. These simulations give a graphical insight into the FSI phenomena that parachute suspension lines experience as they move through the air, and this insight can guide potential changes in the braid architecture to mitigate the vortex-induced vibrations. A well calibrated ICFD model can then be used to perform parametric studies on how changes in braid architecture relate to changes in the vibration response of the suspension line. This paper explores the feasibility of modeling the CPFD experiments with the ICFD solver where the objective is to understand how the vibration response of the line changes as a function of the torsional stiffness of the suspension line.

Introduction

Parachutes are used by the U.S. Army to deliver supplies to personnel in the field. Consisting of a canopy, the braided polyester suspension lines and a payload, GPS-equipped parachute systems autonomously guide supplies to a defined target. When parachutes are in flight, the suspension lines are subjected to a cross-flow of air, resulting in the shedding of periodic vortices. The periodic shedding induces fluctuating drag and lift forces on the suspension line causing it to vibrate which in turn decreases the performance of the parachute system and can challenge the ability of the system to land within a 20-m radius of its target destination. The vibration of the lines also create noise which can be heard for several kilometers, thereby compromising the silent delivery of the payload. This vibration of the suspension lines is a phenomenon known as vortex-induced vibration.

Vortex-induced vibration is of fundamental importance in the study of fluid structure interaction (FSI). It is a destructive phenomenon that can cause problems in a broad variety of engineering systems such as offshore structures, bridges, towers and heat exchangers [1]. Vortex-induced vibration occurs when a fluid interacts with a bluff body, which is a body that has a large aspect ratio compared with the stream-wise dimension [2]. When subjected to a cross-flow, bluff bodies experience flow separation causing a periodic shedding of vortices [3]. The vortex shedding exerts oscillatory forces on the body making it vibrate. These ongoing oscillations that structures endure due to these vibrations can cause undesirable cyclic stresses that compromise the integrity of the structure [4].

To develop an understanding of the relationship between parachute suspension line architecture and vortex-induced vibrations, fluid structure interaction studies can be completed using one of many experimental approaches. One popular experimental approach is Cyber Physical Fluid Dynamics (CPFD). CPFD is an experimental method that combines the use of a physical experiment and a computer control system [5]. For the current research, a servomotor acts as a spring and damper, and a load cell reads the forces experienced by the 3D printed piece that represents a section of the suspension line. The spring constant and damping coefficient are prescribed through the computer program that communicates with the servomotor. The CPFD system can physically simulate the response of the given shape when subjected to cross-flow at the prescribed spring constant and damping coefficient, thereby leading to an understanding of what combination of conditions lessen or increase the vibrational response of the parachute suspension line.

A complimentary or alternative approach to investigate this FSI phenomenon is numerical modeling. The modeling can easily accommodate changes in the parameters of the system such as the surface geometry, Reynolds number and structural stiffnesses; the same as can be done in the CPFD setup. However, a numerical model has advantages over physical models such as the ability to get visualizations of the vortices as they shed from the object and to change part geometry without the need to make a new physical part.

In this paper, the feasibility of using LS-DYNA ICFD to replicate the CPFD experiments for a parachute suspension line is investigated. As a first step to establish the credibility of ICFD to model FSI, a cylinder is subjected to a range of Reynolds numbers, and the results of two-dimensional and three-dimensional models are compared to the classical solutions. With the credibility of the model established, the rounded rectangle geometry from the CPFD test configuration is modeled for two different spring constants that are similar to those used in experimental CPFD studies. The resulting FSI responses of the modeling are concluded to be good representations of the CPFD approach, and ICFD is proposed to be used for exploring how changes in the suspension line architecture can mitigate these vortex-induced vibrations.

Vortex-induced vibration and how it's studied

The first studies of vortex-induced vibration were done experimentally. In 1878, Strouhal studied the cause of a musical note as a wire with a circular cross section was moved through the air. Strouhal found that the frequency of the note changed as the wind velocity and the diameter of the wires changed [6]. This experimental investigation was the start of research on vortex-induced vibrations. In 1908, Henri Bénard continued on Strouhal's studies and used a fixed cylinder in a water tank to demonstrate that the periodic phenomenon that Strouhal was experiencing was due to vortices that were being shed in the trailing flow field [7]. More recent experimental studies have continued to explore the basic flow around a cylinder. In 1978, Sarpkaya looked at the effects of vortex-induced vibration on a rigid cylinder being forced to oscillate in the transverse direction of the stream. The goal of his research was to determine the in- and out-of-phase force components acting on the cylinder and subsequently to predict the dynamic response of an elastic cylinder. The process involved measuring the mean fluid-induced force on the cylinder in the direction of flow for different amplitudes and frequencies of the oscillation of the cylinder. He found that as the amplitude of the forced oscillations increased and as the diameter of the cylinder decreased, the in-line force on the cylinder increased. He also found that lock-in synchronization, a phenomenon that occurs when the shedding frequency reaches the natural frequency of the structure, is present at a shedding frequency lower than that of a stationary cylinder [8]. Through this research Sarpkaya showed that vortex-induced vibration is influenced by more than one factor. Thus, by studying the different parameters of different systems, multiple insights into problems caused by vortex-induced vibration can be learned.

Sometimes the best (and most efficient) way to study vortex-induced vibration as a function of the different influencing factors is through numerical simulation. Numerical simulation can address four different aspects of this problem; the flow field, the structural vibration, the fluid-structure interface and the data analysis [9]. In 2000, a numerical study was done by Evangelinos looking at 3D flow past rigid and flexible cylinders where structural damping was ignored. In these studies, the Reynolds number was ~1000. This choice of Reynolds number was made to ensure the models exhibited a turbulent wake. The span-wise length was varied for the flexible cylinders, and all of these cylinders except one were allowed to move transversely to the direction of flow. Once each of the cylinders experienced the lock-in phenomenon, the lift and drag coefficients were found to be the largest for the rigid cylinders and to be the smallest for the flexible stationary cylinder [10]. This is one example that showed how using numerical simulation makes it easy to focus on certain parameters when studying vortex-induced vibrations as many different factors come into play with how a structure responds to the alternating forces created by vortex shedding.

Methods

Geometry

In the CPFD studies, three geometries were selected to be explored, specifically a cylinder, an ellipse, and a rounded rectangle (Fig. 1). The cylinder was chosen because in the field of FSI it is considered as a prototype of bluff body flow. As a result, it has been well studied and documented for the past 100 years [11]. By analyzing flows past a cylinder and comparing results to documented data, the experimental CPFD studies and numerical simulations can be demonstrated as good approaches to study the vortex-induced vibration of parachute suspension lines. The ellipse was chosen because its shape is more closely related to the suspension line than the cylinder. While it is not as well documented as the cylinder, some studies have looked at flow past an ellipse because it has the general shape of a complex body that allows for the study of the effects of both thickness and angle of attack on flow fields [12]. Lastly, the rounded rectangle was chosen because it is a reasonably simple but still representative shape of the parachute suspension line (Fig. 2). The parachute suspension line in the current study is braided in a cylindrical shape and then flattened with rollers. This process results in a shape as shown in Fig. 2. By investigating the flow over these three shapes, an understanding of how shape contributes to the vortex-induced vibration of the parachute suspension lines can be developed.

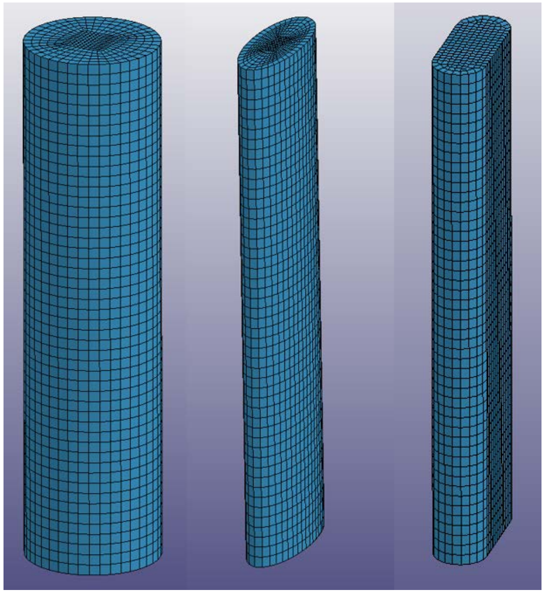	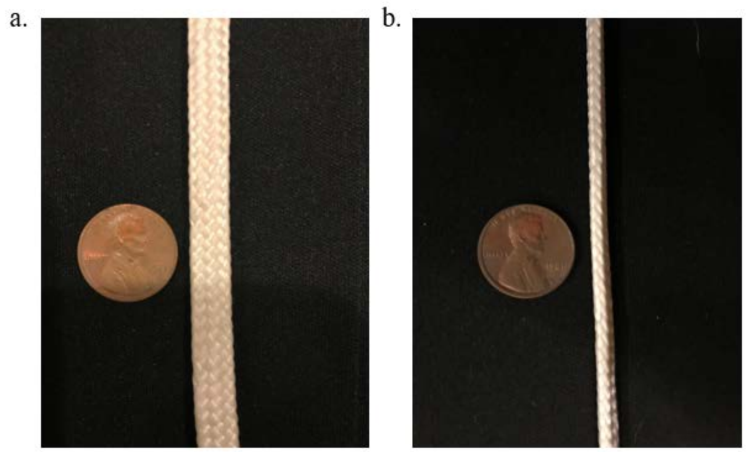
Figure 1: Meshed models of 3D printed cylinder, ellipse, and rounded rectangle used in CPFD studies	Figure 2: Typical suspension line: (a) front view and (b) side view

Modeling Methods

To model the CPFD system, the LS-DYNA incompressible fluid dynamics and implicit solvers were used to perform two-way fluid structure interaction analyses. Three-dimensional models were created to replicate the CPFD system.

The fluid was modeled as a box meshed with tetrahedral elements to define the fluid region. The box consists of an inlet and an outlet for the fluid along the x-axis. The region parallel to the x-axis was prescribed a free-slip condition making it so any fluid that encountered the boundary of that region would be able to flow as if there were no boundary. The interaction point of the fluid region was meshed inside the box and given the same surface geometry as the structure being subjected to the fluid. The interaction point was prescribed a boundary condition of no-slip because that is the point where the fluid and the structure will interact (Fig. 3). The box and interaction point were meshed as surface elements and the keyword *MESH_VOL was used to automatically mesh the volume of the fluid region during the analysis.

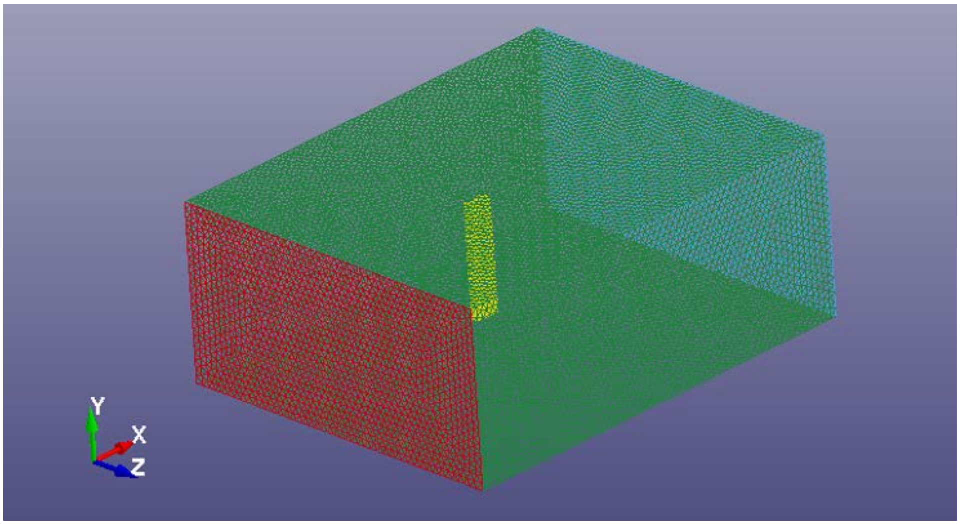

Figure 3: Fluid region where the yellow rectangle in the center is the interaction point.

When assigning the fluid properties to the model, the Reynolds number is needed to replicate the same flow pattern that was occurring in the wind tunnel with the CPFD studies. The CPFD studies used a Reynolds number of around 10,000. To replicate this value, all of the properties of the system in the model replicate those in the wind tunnel except the fluid velocity. The fluid velocity is calculated using the fluid properties and the structural dimension to ensure the Reynolds number of the system is 10,000. The fluid properties were set to mimic those of air, thus the density and dynamic viscosity were prescribed to be air at room temperature. The calculated velocity of 10.5 mph (4.7 m/s) was prescribed to the fluid along the x-axis to mimic the air-flow in the wind tunnel.

There are only two keywords needed to define the FSI problem. The keyword of *ICFD_BOUNDARY_FSI identifies the point at which the fluid and structure will interact. Fig. 3 shows this part in yellow. The keyword of *ICFD_CONTROL_FSI defines the type of coupling that will be used in the FSI problem. There are two types of coupling: two-way and one-way. With two-way coupling, the loads and displacements from the fluid and the structure transfer between the two solvers, i.e. structural and computational fluid dynamics solvers, to obtain a fully coupled FSI problem. One-way coupling is an option where the structural solver can transfer displacements to the fluid solver or the fluid solver can transfer forces to the structural solver. The analysis of this problem was done as a two-way fully coupled FSI problem to replicate how the shape of the structure affects the flow field and how that flow field then in turn exerts forces on that structure.

The finite element model of the structure was created in LS-PrePost® and saved in a file separate from that of the ICFD model. The main body of the structure was created with solid elements that were extruded from a 2D shell mesh of the cross-sectional area. A shell mesh was used on the bottom to provide a rotational degree of freedom to attach a torsional spring. This torsional spring is modeled as a discrete element attached to two nodes. One node is completely fixed in space, and the other is attached to the center node of the shell mesh on the structure (Fig. 4).

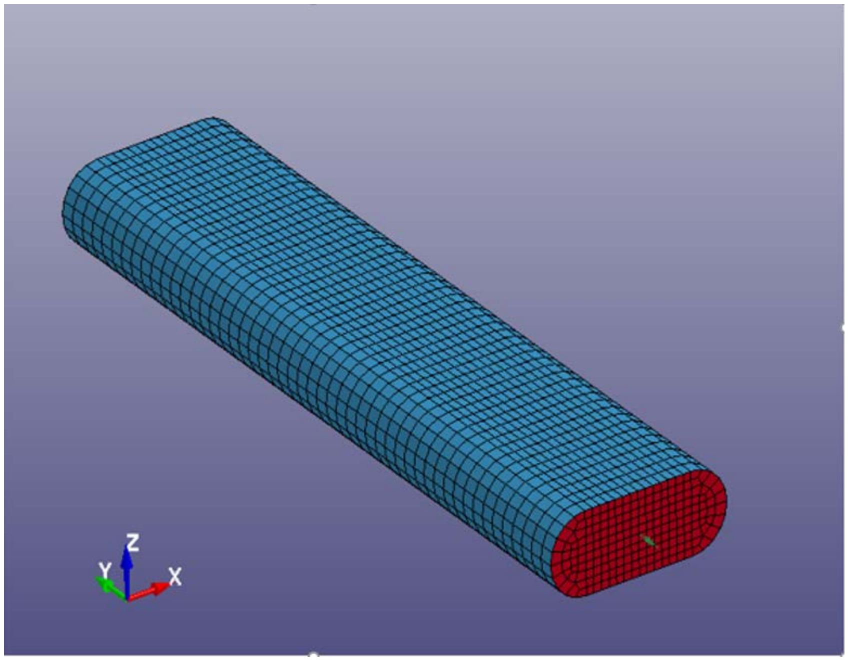

Figure 4: Finite element model of 3D printed rounded rectangle
(blue=solid elements, red=shell elements, and green=discrete spring)

After the structure was completely built, boundary conditions were added to the shell elements. The center node, where the spring is connected, is constrained to only have rotational degrees of freedom (DOFs), i.e. no translational DOFs. The rest of the nodes on the shell elements are only restricted in the y-direction. These boundary constraints allow for the structure to be pinned at that center point such that the entire structucture can rotate freely about that point.

To ensure that a vibrational response of the structure could be induced, a moment about the y-axis was applied to the structure to move it to an angular position of 30° within 0.1s before the fluid velocity was turned on. The structure was held in that position until 0.3s when it was slowly brought back to 0° at 0.4s. The fluid velocity was turned on at 0.2s while the structure was in the 30° position, i.e. when it is a bluff body. This large rotation was done to initialize the vortex shedding. Without such a forced perturbation, the symmetry of the model allowed the flow to pass by the structure without any significant oscillation. In reality, such pure symmetry will unlikely occur.

The material properties are assigned to both the solid and shell elements as *MAT_ELASTIC. The 3D printed pieces that are used in the CPFD expierments are made of acrylonitrile butadiene styrene (ABS), thus properties of ABS were prescribed where the density is 9.7×10^{-5} blobs/in^3 (1.04 g/cm^3), the Youngs Modulus is 330,000 psi (2.28 GPa), and the Poisson's ratio is 0.3. For the spring, the properties were defined using *MAT_SPRING_ELASTIC. This structural model was first run in the implicit solver to demonstate that the model was structurally stable.

Models

When using the numerical approach for the first time, it is helpful to model known cases to show that the methods and parameters that are used in the model yield credible results. For fluid flow studies, the responses of 2D and 3D cylinders have been well documented for a wide range of Reynolds numbers. To give confidence that the approach being used to model the fluid portion of this study was credible, fluid flow models of 2D and 3D cylinders were investigated. Three different Reynolds numbers were considered (100, 1000, and 10K) for both the 2D and 3D versions of the cylinder. Four other 2D models were created with Reynolds numbers of 3, 20, 300K, and 3600K to further establish the credibility of the models. The properties of the fluid and the radius of the cylinder remained the same in all models. The velocity was varied to achieve the different Reynolds numbers needed to change the trailing flow field behind the cylinder. The results were compared with the trends seen in accepted data.

Once it was confirmed that the fluid solver produced credible data for the cylinder, two-way FSI models of the rounded rectangle on a torsional spring were created to simulate the CPFD FSI experiments in ICFD. The two spring constants that are on the lower end of what is expected for a suspension line were studied; 0.1 lb-in/deg (0.0113 N-m/deg) and 10 lb-in/deg (1.13 N-m/deg).

Results

2D and 3D Cylinder Models with changing Reynolds Number

Figs. 5 and 6 show the trailing flow fields associated with equal Reynolds numbers in ICFD simulations of flow over stationary cylinders and the known trailing flow fields, respectively. The models with the Reynolds numbers of 3 and 20 exhibit a flow field that is comparable to their known flow fields (Figs. 6a and b), i.e. showing no flow separation of vortices. The 2D and 3D models were run for Reynolds number of 100, 1000, and 10K (Figs. 5c-e) to see how the results of the 3D simulation compared with that of the 2D simulation as well as comparing their flow fields to known flow fields. The cylinder flow with the Reynolds number of 100 (Fig. 5c) compares well with Fig. 6c. In this flow, vortices shed from the structure at a much lower rate than they do at higher Reynolds numbers. Figs. 5c (2D and 3D) and 6c show a similar trend of vortices shedding. The models shown in Figs. 5d and e were compared with Fig. 6d. With this flow, vortices separate from the structure more often and closer to the structure than they do at lower Reynolds numbers. This quick flow separation is shown in both the 2D and 3D models for Figs. 5d and e, thereby validating those models as well. Lastly, Figs. 5f and g are compared to Figs. 6e and f. The comparison of Figs. 5f and 6e show a similar flow field as there is little vortex shedding, and the flow field is narrower than and not as smooth as it was in Figs. 5a and b. In Figs. 5g and 6f, both flow fields have regained the vortex shedding; however, the flow is not as smooth as in Figs. 5c-e, and that can be seen in both images.

When comparing the 2D and 3D cases of the fluid flow over the cylinder, some variations can be observed. While both models shed vortices from the cylindrical boundary for the given Reynolds number, the flow fields are slightly different. This difference is a result of the 3D model the no-slip boundary being completely submerged in the fluid, allowing the fluid to run over the top and bottom of the boundary. This boundary condition creates edge effects which can perturb the trailing flow field and make it look slightly different than the 2D model.

Overall the data from the models compared well with accepted data for given Reynolds numbers. While 2D and 3D flow fields do not agree perfectly with each other, they are similar enough that the 3D boundary definitions should have little effect on the study at hand. In the future, it should be noted that adding separation plates in the model or restricting the flow so that it can only see the mid-section of the structure would improve the correlation between the 2D and 3D cylinder models.

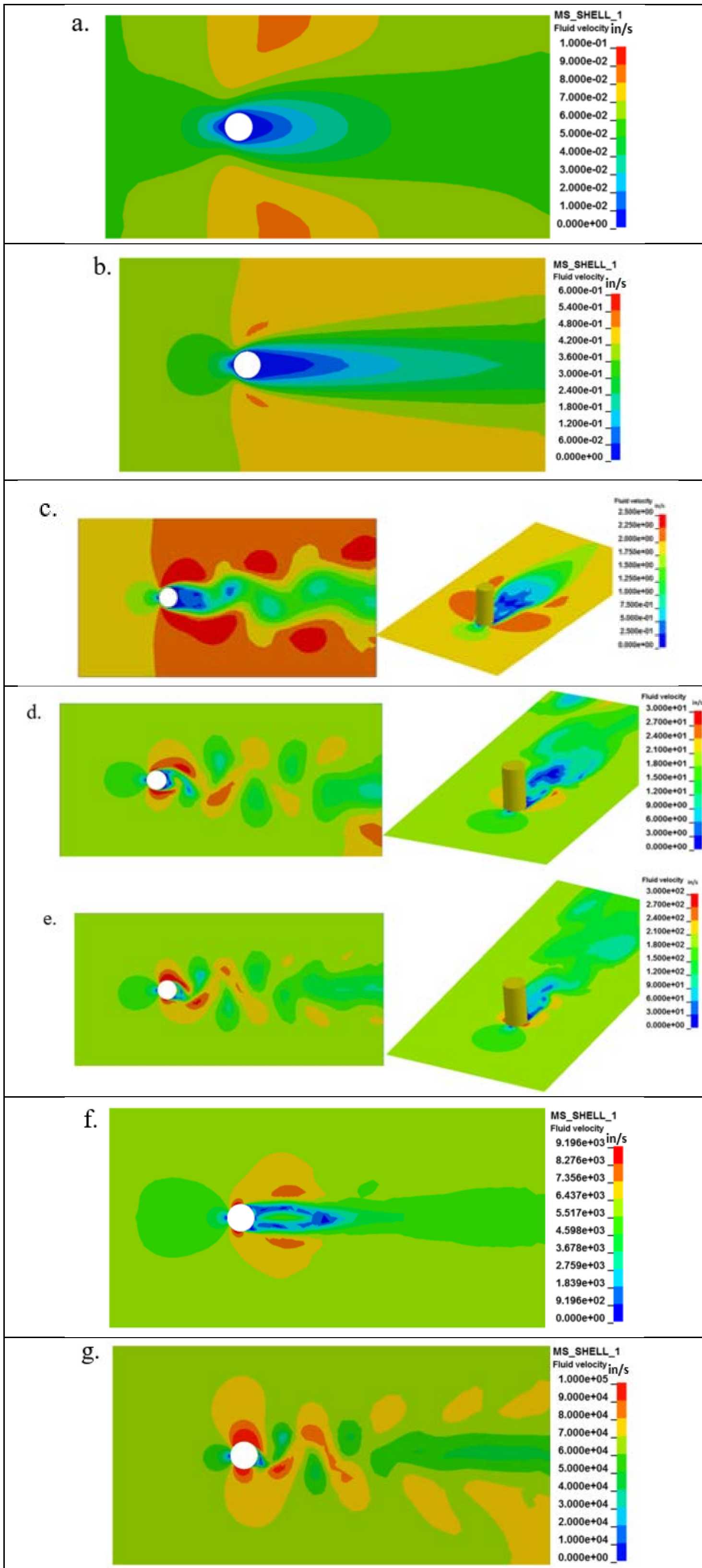

Figure 5: 2D and 3D ICFD models of cylinders at different Reynolds numbers: (a) Re=3 (b) Re=20 (c) Re=100 (d) Re=1,000 (e) Re= 10,000 (f) Re= 300,000 (g) Re=3,600,000

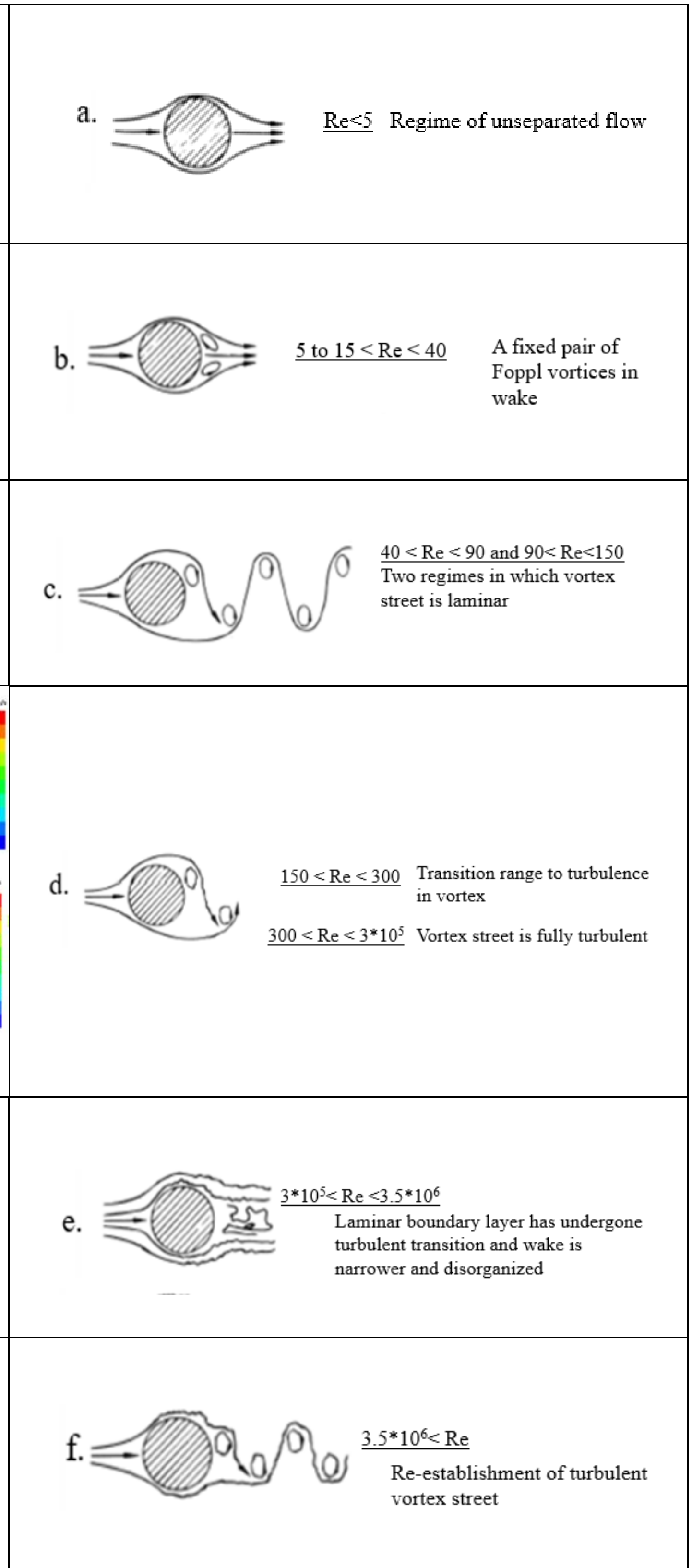

Figure 6: Regimes of fluid flow across a smooth cylinder[13]

3D FSI Models with Varying Spring Constants

Modeling the FSI of the rounded-rectangle at different spring constants can give insight into the relationship between the torsional stiffness and the vibrational response of the suspension line. This modeling will also allow for the evaluation of the feasibility of modeling the CPFD system to compare modeled results to experimental results for the purposes of validation.

Fig. 7 shows the change in angle of the rounded rectangle as a function of time for the two spring constants, and Fig. 8 shows the velocity plots at three different times for the case of k=0.1 lb-in/deg. The data in Fig. 7 start from when the rounded rectangle was brought from the 30^o (Fig. 8a) position back to the 0^o (Fig. 8b) position at 0.4s. When comparing torsional stiffnesses of each of the models, the frequency and amplitude of the vibrational response was examined. It was discovered that as the torsional stiffness increases the frequency increases (Table 1) and the amplitude decreases (Fig. 7a and b). In each of these time responses, the amplitude of the vibration decreases with time. The initially high amplitudes are most likely a result of the inertial forces that are present after the load on the structure is released. The amplitude decreases over time as a consequence of the damping by the viscosity of the fluid. It is assumed that the amplitude will eventually reach a steady-state value. This steady-state condition will be explored in the near future by allowing the models to run for more than 1.6s. Fig. 8 gives a graphical representation of these responses at three points in time when k=0.1 lb-in/deg (results for k=10 lb-in/deg look similar). In the 30^o position, the initiation of the shedding of vortices can be seen in Fig. 8a. The vortices continue to shed as the structure is brought back to the 0^o position (Fig. 8b). The shedding vortices then continue to induce the vibration response of the structure.

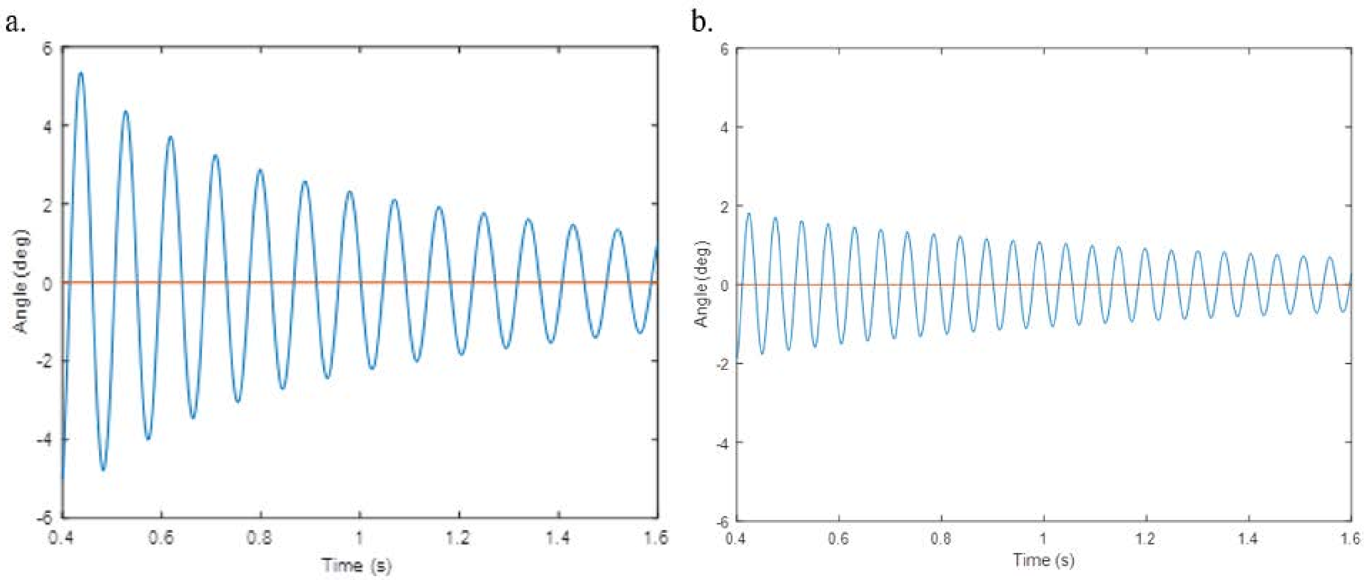

Figure 7: Angular Position vs. Time of the Rounded Rectangle where (a) k=0.1 lb-in/deg and (b) k=10 lb-in/deg

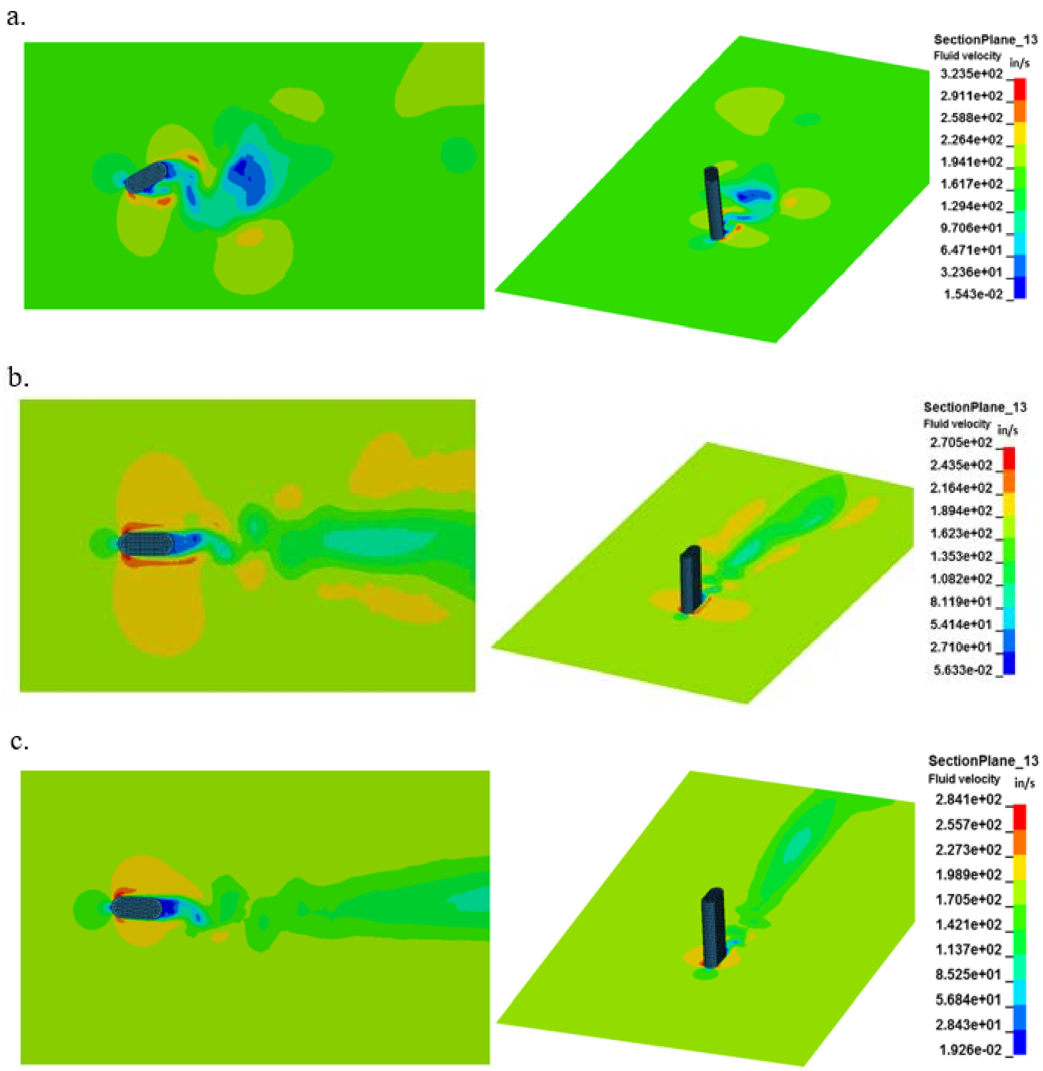

Figure 8: Velocity plots of the FSI of the rounded-rectangle when k=0.1 lb-in/deg (a) held at a 30° angle (b) brought back to the 0° position (c) and allowed to freely oscillate

The results shown in Fig. 7 and Table 1 confirm the ability of the LS-DYNA ICFD solver to be able to model CPFD experiments. The increase in frequency and decrease in amplitude as the spring stiffness is increased is a trend that is seen in the CPFD experiments. From this small numerical study, it can be concluded that it is possible to model CPFD experiments using ICFD. Future work in this area will study the FSI of the cylinder and the ellipse as well as the rounded rectangle at torsional stiffnesses up to 100 lb-in/deg (11.3 N-m/deg) to see the variations in responses. These studies will then lead to further insight on the cause of the vortex-induced vibration of the parachute suspension lines and ultimately how to alleviate them.

Table 1: Frequency of the Rounded Rectangle at two different spring constants

Spring Constant (lb-in/deg)	**Rounded Rectangle (Frequency Hz)**
0.1	11
10.0	19

Conclusions

This paper discussed the feasibility of modeling FSI response of CPFD experiments on a parachute suspension line with the LS-DYNA ICFD and implicit solvers. First, ICFD models of fluid flow over a cylinder were run at varying Reynolds numbers for 2D and 3D simulations and compared to known flow fields with the same Reynolds numbers. The 2D simulations were comparable to the well-accepted responses for a cylinder subjected to cross-flow. The comparison of 2D and 3D simulations showed a slight difference in the flow field, and this difference is explained by the edge effects of the top and bottom of the submerged no-slip boundary. However, the flow fields were deemed similar enough to be able to demonstrate the feasibility of modeling the CPFD experiments of the suspension line in ICFD. In the future, the incorporation of separation plates or a way to constrict the flow to the mid-section of the structure should be considered to avoid edge effects. FSI studies were then run on a rounded rectangle with two different spring constants to see how torsional stiffness affected vortex-induced vibration. It was found that as torsional stiffness increases, frequency increases and amplitude decreases. This trend was also observed in the CPFD studies, thereby demonstrating that the LS-DYNA FSI analysis is able to model the CPFD experiments. Future work on this project is to replicate results that are seen in CPFD experiments to validate the model and eventually to study how changes in torsional stiffness and changes in surface geometry affect the vortex-induced vibration of parachute suspension lines. Ultimately, the modeling will be able to help discover what parameters can mitigate the vortex-induced vibration of the suspension lines.

Acknowledgements

The authors acknowledge the U.S. Army Natick Soldier Research, Development and Engineering Center for its support of this work through Cooperative Agreement W911QY-15-2-0002.

References

1. C.Y.Zhou, R.M.C.S., K.Lam, *Vortex-Induced Vibrations on Bluff Bodies in a Cross Flow*, in *ASME Fluids Engineering Division Summer Meeting*. 1998, FEDSM: Washington D.C.
2. Païdoussis, M.P., S.J. Price, and E. de Langre, *1. Introduction*, in *Fluid-Structure Interactions - Cross-Flow-Induced Instabilities*. Cambridge University Press.
3. Shaughnessy, E.J., Jr., I.M. Katz, and J.P. Schaffer, *14.4.4 Bluff Bodies*, in *Introduction to Fluid Mechanics (OUP Edition)*. Oxford University Press.
4. Janardanan, A., *Reducing Vortex-Induced Vibration of Drilling Risers with Marine Fairing*, in *Naval Architecture and Marine Engineering*. 2014, University of New Orleans: ScholarWorks@UNO. p. 73.
5. Mackowski, A.W. and C.H.K. Williamson, *Developing a cyber-physical fluid dynamics facility for fluid–structure interaction studies.* Journal of Fluids and Structures, 2011. **27**(5): p. 748-757.
6. Wesfreid, J.E., *Henri Bénard: Thermal convection and vortex shedding.* Comptes Rendus Mécanique, 2017. **345**(7): p. 446-466.
7. Norberg, C., *Effects of Reynolds number and a low-intensity freestream turbulence on the flow around a circular cylinder.*
8. Gabbai, R.D. and H. Benaroya, *An overview of modeling and experiments of vortex-induced vibration of circular cylinders.* Journal of Sound and Vibration, 2005. **282**(3): p. 575-616.
9. So, R.M.C. and X.Q. Wang, *VORTEX-INDUCED VIBRATIONS OF TWO SIDE-BY-SIDE EULER-BERNOULLI BEAMS.* Journal of Sound and Vibration, 2003. **259**(3): p. 677-700.
10. Evangelinos, C., D. Lucor, and G.E. Karniadakis, *DNS-DERIVED FORCE DISTRIBUTION ON FLEXIBLE CYLINDERS SUBJECT TO VORTEX-INDUCED VIBRATION.* Journal of Fluids and Structures, 2000. **14**(3): p. 429-440.
11. Noack, B.R., *On the flow around a circular cylinder. Part I: Laminar and transitional regime.* ZAMM - Journal of Applied Mathematics and Mechanics / Zeitschrift für Angewandte Mathematik und Mechanik, 1999. **79**(S1): p. 223-226.
12. R. Mittal, S.B., *Direct Numerical Simulation of Flow Past Elliptic Cylinders.* Journal of Computational Physics, 1995. **124**: p. 351-367.
13. Belvins, R.D., *Flow Induced Vibration 2nd Edition*. 1990: Krieger Publishing Company.